Int Nano Lett (2015) 5:141–146
DOI 10.1007/s40089-015-0147-6

ORIGINAL ARTICLE

Solution combustion synthesis using Schiff-base aluminum complex without fuel and optical property investigations of alumina nanoparticles

Mehdi Salehi[1] · **Ehsan Arabsarhangi**[1]

Received: 12 December 2014 / Accepted: 13 April 2015 / Published online: 1 May 2015

Abstract Synthesis of alumina nanomaterials via a solution combustion technique using Schiff base aluminum (III) complex at 820 and 950 °C for 4 h was performed successfully. The synthesis procedure was performed using the complex in the absence and presence of urea and glycine as fuel for comparison. The obtained data showed that the procedure without using fuel resulted in a better phase and morphology. To investigate the phase formation, powder X-ray diffraction technique was used. Also, SEM micrographs were used to investigate the morphology of the obtained materials. The optical properties of the obtained materials were studied by FTIR spectra. According to the PXRD data, it was found that with annealing at 950 °C, the phase formation of the obtained materials showed cubic crystal structure with cell parameter $a = 3.14$ Å for gamma phase. Also, by annealing at 820 °C using fuels for 4 h, the main phase was found to be in gamma.

Keywords Alumina · Solution combustion · Schiff base · Nanomaterial

Introduction

Aluminum oxide (Al_2O_3) is one of the most important industrial materials, which is widely used as adsorbent [1], catalyst [2], catalyst support [3, 4], functional ceramics [5, 6], reinforcement for composite material abrasives [7], ceramic materials, imitation jewelry [8, 9], sorbents and catalysts [10], dosimeters [11], and so on because of its low-cost, good thermal stability, and high-specific surface area [12, 13]. Moreover, it is a major ingredient for the preparation of complex oxides because of its promising luminescent [14], thermoluminescent [15], and scintillation properties [16].

Several procedures have reported the synthesis of different alumina nanomaterial phases such as precipitation [17], spray pyrolysis [18], sol–gel reactions [19], methods utilizing different surfactants as a template [20], formation of solid precursors of aluminum hydroxides or oxyhydroxides with various compositions, and crystallinity [21]. The aim of this article is to investigate the preparation of nano-alumina by a novel solution combustion method using a complex and without using fuel. To compare the synthesis procedure with the condition in the present fuel, different fuels were used at a temperature of 820 °C. So, to the best of our knowledge, the investigation of synthesis of Al_2O_3 from this method and using the raw materials has not been reported.

Materials and methods

Synthesis of the ligand *N*,*N*′-Bis(salicylidene)ethylenediamine (salen)

Certain amounts of ethylenediamine (en) and salicylaldehyde were mixed together in a 1:2 molar ratio. The obtained precipitate was dissolved in a hot ethanol and then filtered.

Synthesis of complex $[Al(salen)_3(H_2O)_2]NO_3$

Certain amounts of aluminum nitrate and the synthesized ligand in a 1:2 molar ratio were used. First, the aluminum nitrate and the ligand were dissolved in a hot ethanol

✉ Mehdi Salehi
msalehi@semnan.ac.ir

[1] Department of Chemistry, Semnan University, Semnan, Iran

separately, and the aluminum solution was added to the ligand solution slowly. The obtained material resembles a white precipitate. The obtained material was filtered and washed with ethanol. Yield: 65 %. Analysis calculated for $C_{16}H_{18}AlN_3O_7$ (%): C, 49.11; H, 4.64; N, 10.74. Found (%): C, 48.55; H, 4.57; N, 10.65.

Synthesis of nano-alumina

To obtain a clear solution, a certain amount of the synthesized complex was dissolved in distilled water. Also, two solutions using the two different fuels were prepared. The solution was heated at 60 °C to obtain a gel. Then, the gel was annealed at 450 °C for 4 h. The obtained materials were in black-like form. To eliminate the residual organic components, the powders were heated more at 820 or 950 °C for 4 h.

Results and discussion

Powder X-ray diffraction (PXRD) analysis

Phase characterization of the obtained materials was investigated using PXRD technique with CuKα radiation at the range of 10°–90° and the step of 0.05°. Figures 1, 2 and 3 show the X-ray diffraction (XRD) patterns of the obtained alumina nanomaterials. Figure 1 shows the XRD pattern of the obtained material without using any fuel to synthesize alumina annealed at 950 °C for 4 h. As shown in Fig. 1, the main phase for the synthesized material is beta (JCPDScard number: 100414) and gamma (JCPDS card number: 011307) nano-alumina. Also, Fig. 2 shows the PXRD pattern of the obtained material using urea as fuel for the synthesis of nano-alumina at 820 °C for 4 h. The figure shows that the main phase is actually gamma

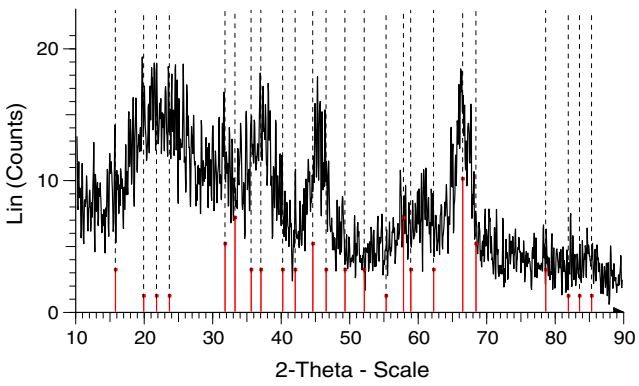

Fig. 1 PXRD pattern of the synthesized a multi-phase beta and gamma nano-alumina via a solution combustion method without using fuel at 950 °C for 4 h

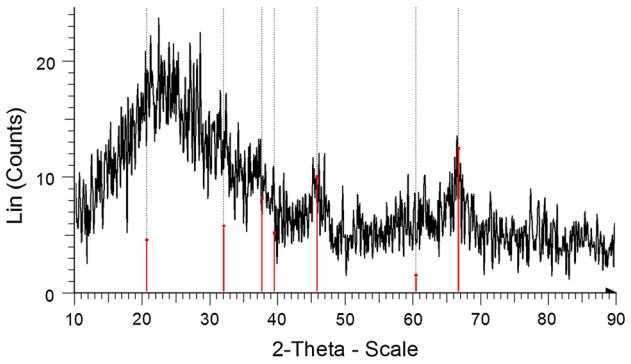

Fig. 2 PXRD pattern of the synthesized gamma nano-alumina via a solution combustion method using urea as fuel at 820 °C for 4 h

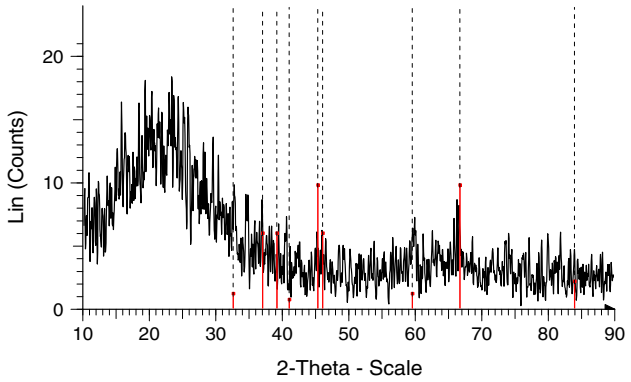

Fig. 3 PXRD pattern of the synthesized gamma nano-alumina via a solution combustion method using glycine as fuel at 820 °C for 4 h

(JCPDS card number: 040858) nano-alumina. Moreover, Fig. 3 shows the PXRD pattern of the obtained material using glycine as fuel to synthesize alumina at 820 °C for 4 h. The figure shows that the main phase is gamma (JCPDS card number: 291486) nano-alumina. As shown in Figs. 1, 2 and 3, it is clear that with using fuel for the synthesis of nano-alumina, the obtained phase is nearly pure gamma alumina. However, when the reaction was performed without using any fuel, the obtained phase was a mixture of beta and gamma nano-alumina. But the ratio of gamma to beta phase was 0.89. It shows that the ratio of gamma phase in the synthesized nanomaterial is about 45 %.

Morphology analysis

Figure 4 shows the scanning electron microscopic (SEM) images of the synthesized nanomaterials via a combustion method without using fuel, annealed at 950 °C for 4 h. Figure 4a shows the low-magnification image of the synthesized material. It is clear that the sample is in a porous-like structure. It shows that the porosity distribution is nearly homogeneous. Figure 4b shows that the porosity is

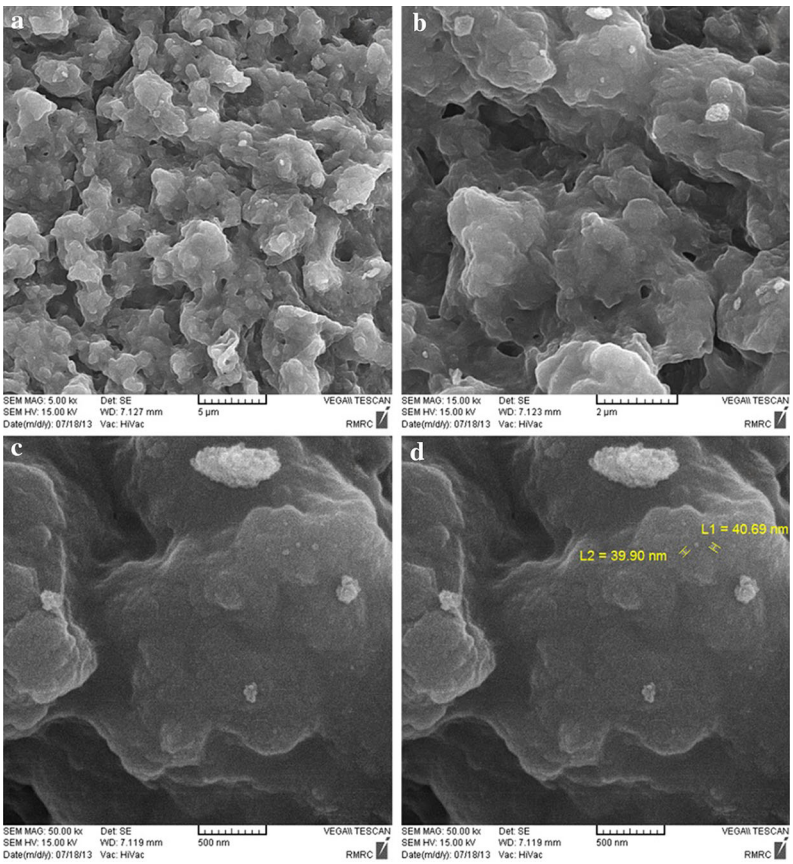

Fig. 4 SEM images of the obtained materials from the combustion method without using fuel annealed at 950 °C for 4 h

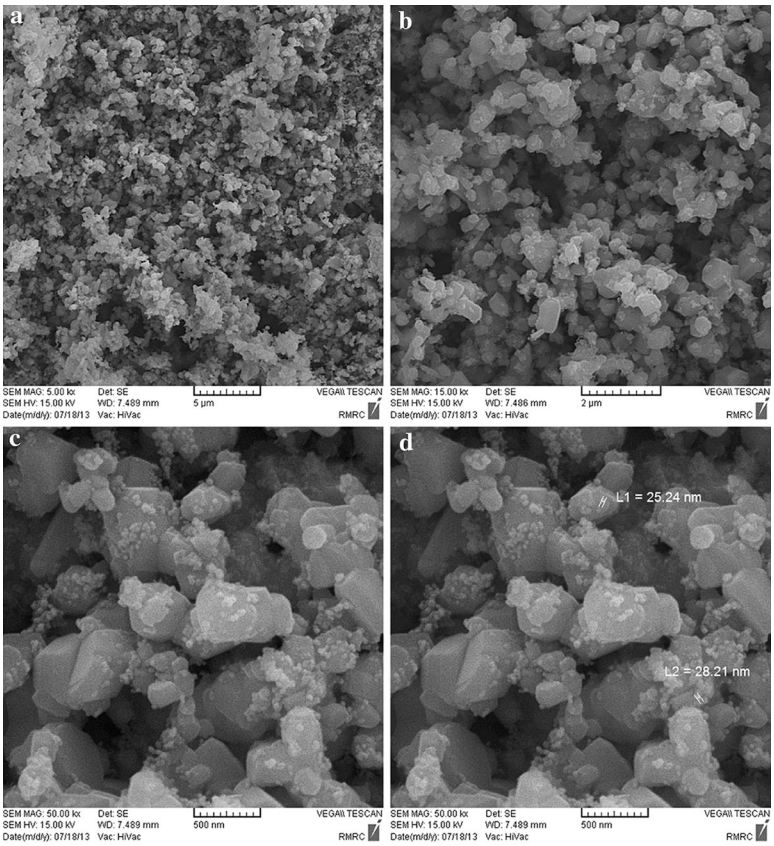

Fig. 5 SEM images of the obtained materials from the combustion method without using fuel annealed at 820 °C for 4 h

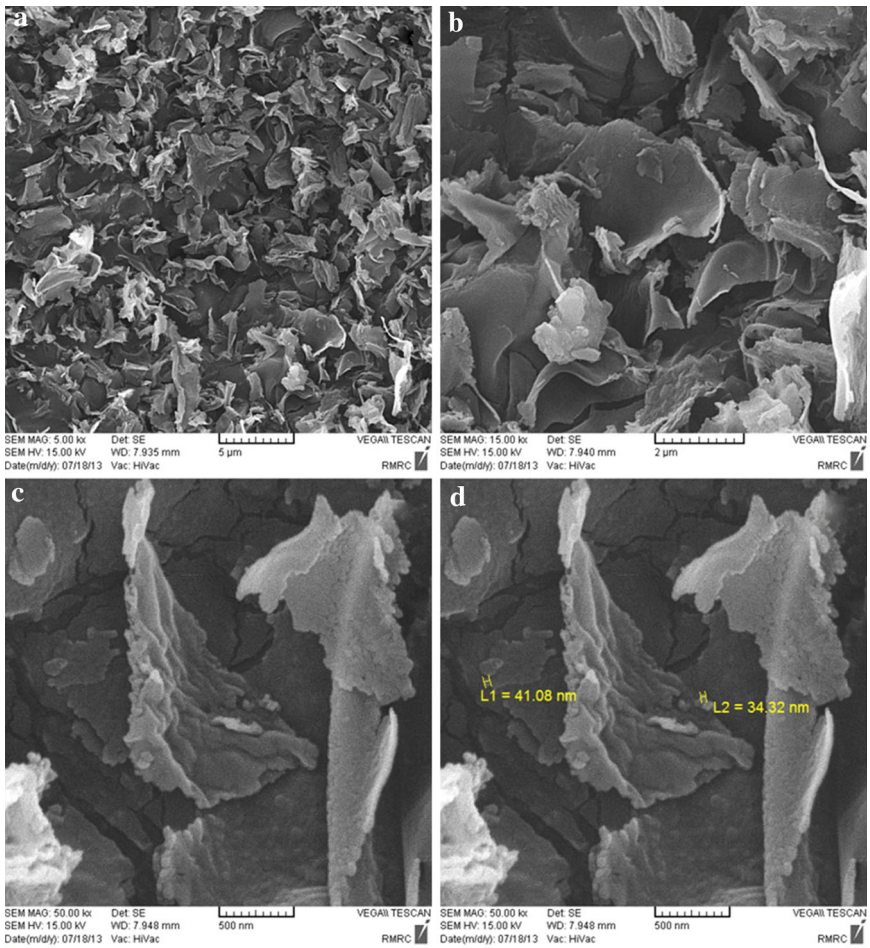

Fig. 6 SEM images of the obtained materials from the combustion method using urea as fuel annealed at 820 °C for 4 h

in micro-porosity range. It shows that the porosity diameter is in a range of about 50–200 nm. Figure 4c and d shows the high-magnification image of the synthesized nanomaterials. It is clear that there are small particles, as uncus, on the synthesized materials. It shows that the particle sizes are in a range of about 40–200 nm in diameter.

Figure 5 shows the SEM images of the synthesized nanomaterials via a combustion method without using fuel, annealed at 820 °C for 4 h. Figure 5a shows the low-magnification image of the synthesized material. It is clear that the sample is in a grain-like structure. It shows that the size and morphology distribution is nearly homogeneous. Figure 5b shows that there is porous structure in the analyzed sample. Figure 5c shows that the porosity size is in micro-porosity range. It also shows that the porosity diameter is in a range of about 100–150 nm. Figure 5d shows the high-magnification image of the synthesized nanomaterials. It is clear that the large particle's diameter is in the range of about 200–500 nm, and the small particles, as uncus on the synthesized materials, are in a range of about 25–50 nm in diameter.

Figure 6 shows the SEM images of the synthesized nanomaterials via a combustion method using urea as fuel, annealed at 820 °C for 4 h. Figure 6a and b shows the low-magnification image of the synthesized material. It is clear that the sample is in a flake-like structure. It shows that the size and morphology distribution is nearly homogeneous. Figure 6c shows that the size of the thickness of the flakes is about 50–80 nm. Figure 6d shows the high-magnification image of the synthesized nanomaterials. It is clear that the length of the flakes is in the range of about 2–3 μm.

Figure 7 shows the SEM images of the synthesized materials via a combustion method using glycine as fuel, annealed at 820 °C for 4 h. Figure 7a and b shows the low-magnification image of the synthesized material. It is clear that the sample is a porous-like structure with small particles on the sample. It shows that the size and morphology distribution is nearly homogeneous. Figure 7c and d shows the high-magnification image of the synthesized material. It is clear that the size of the diameter of the pores is in the range of about 70–100 nm, and the particle sizes are in a range of about 30–50 nm.

Figure 8a–b shows the Fourier transform infrared (FTIR) spectra of the synthesized nanomaterials via a combustion method at different conditions. The FTIR spectrum of the synthesized nanomaterial annealed at

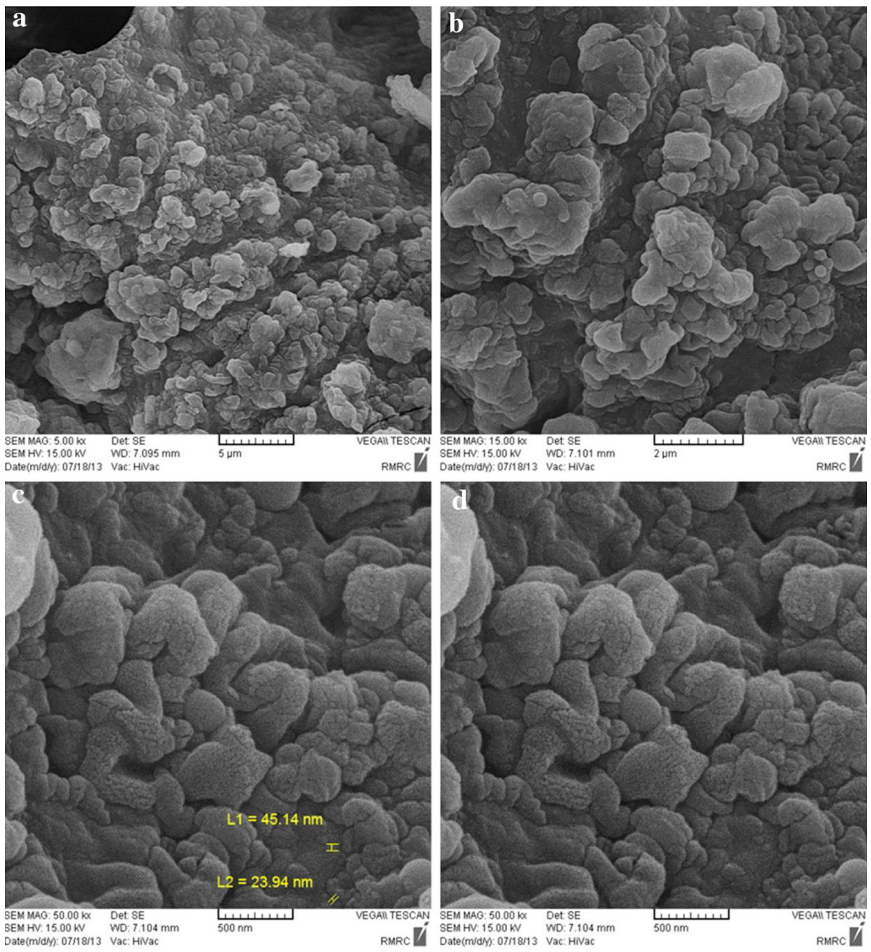

Fig. 7 SEM images of the obtained materials from the combustion method using glycine as fuel annealed at 820 °C for 4 h

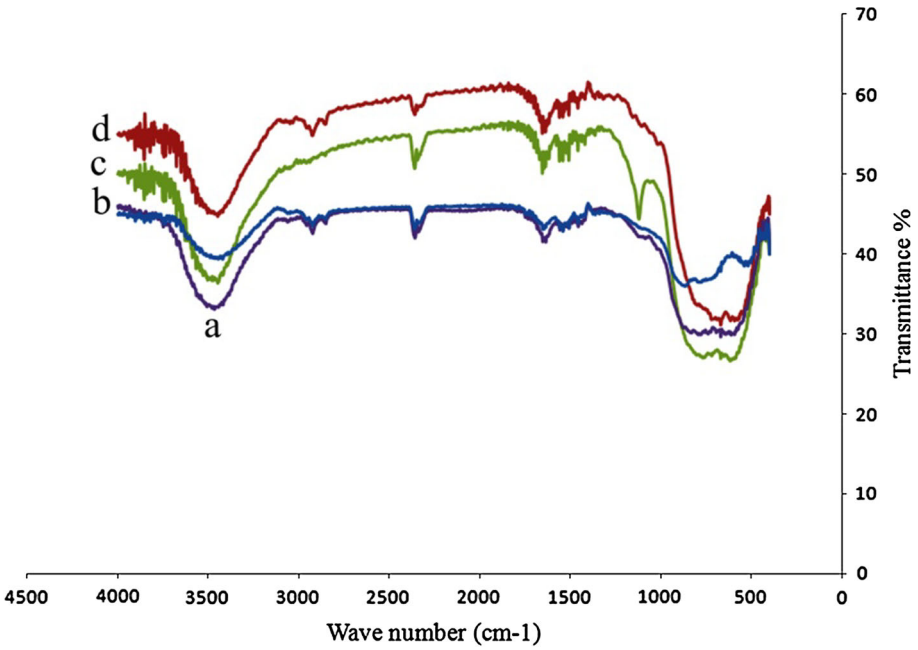

Fig. 8 FTIR spectrum of the synthesized nanomaterial via a combustion method without using any fuel at *a* 820 °C, *b* 850 °C, *c* using urea as fuel at 820 °C and *d* using glycine as fuel at 820 °C for 4 h

950 °C is shown in Fig. 8. The peaks at 1625–1650 cm^{-1} are assigned to the bending vibrations of the hydroxide. The weak peaks at 1508 and 2340 cm^{-1} are assigned to nitrate and carbonate. Figure 8b shows the FTIR spectrum of the synthesized nanomaterial annealed at 820 °C for 4 h. The peaks at 400 to 900 cm^{-1} are assigned to Al–O vibrations [22]. The peaks at 500–570 cm^{-1} are assigned to AlO_6, and the peaks at 675–775 cm^{-1} are assigned to AlO_4. Also, the peaks at 1635 cm^{-1} are assigned to the bending vibrations of hydroxide vibrational mode, and the peak around 3480 cm^{-1} is assigned to the stretching vibration of hydroxide.

Conclusion

Synthesis of nano-alumina with different conditions was performed successfully. PXRD data showed that the main phase for all of the synthesized nanomaterials was gamma. It showed that the nanomaterials were synthesized with high purity. SEM images showed that the synthesized nanomaterials were in different morphology depending on the synthesis procedure. It is clear that reaction temperature is a main factor on the synthesized nanomaterial's morphologies. However, it showed that the fuel type is also an important factor on the morphology of the synthesized nanomaterials. The SEM images showed that the morphology of the obtained materials is in the form of porous particle and irregular particle shape. FTIR spectra of the nano-alumina were investigated in different synthesis conditions.

Acknowledgments We thank Semnan University for supporting this study.

References

1. Mahmoud, M.E., Osman, M.M., Hafez, O.F., Elmelegy, E.J.: Adsorption equilibrium and kinetics of fluoride on sol–gel-derived activated alumina adsorbents. Colloid Interface Sci. **349**, 307–313 (2010)
2. Gong, S.F., Shinozaki, A., Shi, M.L., Qian, E.W.: Hydrotreating of jatropha oil over alumina based catalysts. Energy Fuels **26**, 2394–2399 (2012)
3. Gaudet, J.R., Riva, A., Peterson, E.J., Bolin, T., Datye, A.K.: Improved low-temperature CO oxidation performance of Pd supported on La-stabilized alumina. Am. Chem. Soc. Catal. **3**, 846–855 (2013)
4. Puron, H., Pinilla, J.L., Berrueco, C., Fuente, J.A., Millan, M.: Hydrocracking of maya vacuum residue with NiMo catalysts supported on mesoporous alumina and silica–alumina. Energy Fuels **27**, 3952–3960 (2013)
5. Zhou, X., He, X., Su, B.: Ultrasonic synthesis of the microporous metal–organic framework $Cu_3(BTC)_2$ at ambient temperature and pressure: An efficient and environmentally friendly method. Mater. Lett. **63**, 830–832 (2009)
6. Qi, Y.E., Zhang, Y.S., Fang, Y., Hu, L.T.: Design and preparation of high-performance alumina functional graded self-lubricated ceramic composites. Compos Part B Eng. **47**, 145–149 (2013)
7. Zhu, Z.F., Liu, H., Sun, H.J., Yang, D.: PEG-directed hydrothermal synthesis of multilayered alumina microfibers with mesoporous structures. Microporous Mesoporous Mater. **123**, 39–44 (2009)
8. Furukawa, M.: Alumina ceramic tools. Am. Ceram. Soc. Bull. **62**, 1384–1387 (1983)
9. Uhlmann, D.R., Teowee, G.: Sol-gel science and technology: current state and future prospects. J. Sol–Gel. Sci. Technol. **13**, 153–162 (1998)
10. Cejka, J., Kooyman, P.J., Vesela, L., Rathousky, J., Zukal, A.: High-temperature transformations of organised mesoporous alumina. Phys. Chem. Chem. Phys. **4**, 4823–4829 (2002)
11. Cejka, J.: Organized mesoporous alumina: synthesis, structure and potential in catalysis. Appl. Catal. A **254**, 327–338 (2003)
12. Das, K., Ray, S.S., Chapple, S., Wesley-Smith, J.: Mechanical, thermal, and fire properties of biodegradable polylactide/boehmite alumina composite. Ind. Eng. Chem. Res. **52**, 6083–6091 (2013)
13. Renuka, N.K., Shijina, A.V., Praveen, A.K.: Mesoporous γ-alumina nanoparticles: synthesis, characterization and dye removal efficiency. Mater. Lett. **82**, 42–44 (2012)
14. Muthe, K.P., Kulkarni, M.S., Rawat, N.S., Mishra, D.R., Bhatt, B.C., Singh, A., Gupta, S.K.: Melt processing of alumina in graphite ambient for dosimetric applications. J. Lumin. **128**, 445–450 (2008)
15. Peng, C.H., Hwang, C.C., Hsiao, C.S.: Judd-Ofelt analysis and optically stimulated two-photon absorption of Yb3+-doped $NdAl_3(BO_3)_4$ single crystals. J. Alloys Compd. **491**, 29–32 (2010)
16. Henaish, B.A., El-Agrami, A.M., Abdel-Fattah, W.I., Osiris, W.G.: Characteristic thermoluminescence of gamma-irradiated alumina ceramics doped with some alkali metals. Radiat. Phys. Chem. **44**, 73–77 (1994)
17. Ogino, H., Yoshikawa, A., Nikl, M., Krasnikov, A., Kamada, K., Fukuda, T.: Growth and scintillation properties of Pr-doped $Lu_3Al_5O_{12}$ crystals. J. Cryst. Growth **287**, 335–338 (2006)
18. Kim, J.H., Jung, K.Y., Park, K.Y., Cho, S.B.: Characterization of mesoporous alumina particles prepared by spray pyrolysis of $Al(NO_3)_2$ $9H_2O$ precursor: effect of CTAB and urea. MicroporousMesoporous Mater. **128**, 85–90 (2010)
19. Jayaraman, V., Gnanasekaran, T., Periaswami, G.: Low-temperature synthesis of β-aluminas by a sol–gel technique. Mater. Lett. **30**, 157–162 (1997)
20. Aguado, J., Escola, J.M., Castro, M.C.: Influence of the thermal treatment upon the textural properties of sol–gel mesoporous γ-alumina synthesized with cationic surfactants. MicroporousMesoporous Mater. **128**, 48–55 (2010)
21. Zhang, X., Honkanen, M., Levänen, E., Mäntyla, T.: Transition alumina nanoparticles and nanorods from boehmite nanoflakes. J. Cryst. Growth. **310**, 3674–3679 (2008)
22. Nemade, K.R., Waghuley, S.A.: Low temperature synthesis of semiconducting α-Al_2O_3 quantum dots. Ceram. Int. **40**, 6109–6113 (2014)